Hybrid Visible Imaging and Near-infrared Optical Spectroscopy with Smartphone Image Sensor using Bioinspired Nanostructures

Radwanul H. Siddique[1], Daniel Assumpcao[1,2], Hyochul Kim[2], YoungGuen Roh[2], Tze Ching Fung[1], Hyuck Choo[3], Yibing Michelle Wang[1]

[1]Meta Vision Lab, Samsung Semiconductor, Inc., 2 N Lake Ave, Ste. 240, Pasadena, California 91101, USA.
[2]Advanced Sensor Lab, Device Research Center, Samsung Advanced Institute of Technology (SAIT), Suwon, 16678, Republic of Korea.
[3]System LSI Division, Samsung Electronics Co., Ltd., Hwaseong, Gyeonggi-do, 18448, Republic of Korea.
Author e-mail address: r.siddique@samsung.com

Abstract: Optical spectrometers integrated into smartphones can be vital for numerous futuristic consumer applications that require on-site materials detection and sensing. However, high performance optical spectrometer is difficult to miniaturize due to inherent limitations of light dispersion. We propose and demonstrate an ultracompact spectrometer that accomplishes simultaneous wide angle visible imaging and near-infrared (NIR) spectroscopy on a single conventional CMOS image sensor, allowing integration into pre-existing handheld or smartphone cameras. The core dispersive element is based on a bioinspired approach that combines disordered scattering nanostructures with ordered resonances from distributed Bragg reflector and achieves a large, and angle-independent dispersion with a footprint of only 0.01 mm^3. Using the ultracompact spectrometer with total track length below 5 mm, we demonstrate 200 nm NIR spectroscopy with sub-5 nm spectral resolution, an angular tolerance of 30°, and high throughput sensing and detection.

I. Introduction

Optical spectroscopy has been a key characterization technique in a variety of settings from scientific study to industrial and healthcare applications [1]. Traditional spectrometers use a dispersive element such as a diffraction grating or prism to achieve an angle-dependent light dispersion, accompanied with focusing optics that focus the incoming light on the detector. This combination of free space elements results in good performance at the expense of bulky size [1]. However, in order to proliferate its use and envision regular consumers to achieve in-situ material detection and sensing, it is imperative to realize high-performance ultracompact spectrometers integrated into smartphones [2]. In addition to the traditional performance parameters such as high resolution, high throughput, and large spectral range, it is vital that these handheld spectrometers also have a wide acceptance angle for increasing the throughput of the devices and allowing it to tolerate more misalignment between spectrometer and the spectroscopy target.

Attempts have been made to directly miniaturize grating-based spectrometers using micro-optical components [3, 4]. However, combining micro-optical components of inferior quality and the intrinsic loss of spectral resolution due to inevitable shorter path lengths have led to poor resolutions in compact form (still over few mm^3). A dielectric metasurface-based spectrometer were demonstrated to alleviate these issues, but its angle dependence further exacerbated the intrinsic narrow operation angle (2°) of grating spectrometers [5].

Due to this unsuitability, a variety of novel schemes for realizing on-chip compact spectroscopy have been investigated using integrated photonics [6–8]. However, weak free space to on-chip coupling has significantly limited the throughput and remote applications with these devices. Another heavily investigated method combines an array of filters, typically bandpass filters centered at different wavelengths, directly on a detector array, leading to a compact form factor [9–14]. Despite the compactness of these devices, the efficiency is limited by the filtering operation and the input angle is limited by shifts in the resonance, leading to poor signals and angular tolerances often below 2° [11]. Moreover, filter arrays based on absorption using photonic crystals [12], quantum dots [13] and nanowires [14], are not compatible with standard CMOS microfabrication, limiting their use in existing technological platform.

In this work, we have drawn inspiration from the spectrally tunable interlaced facet lenses found on the compound eyes of long-legged flies [15] to realize a wide-angle, high-resolution light-dispersing structure for ultracompact photo-spectrometry. This bio-inspired dispersive element (BioDE) comprises different sets of 1-dimensional random nanostructures positioned on top of a distributed Bragg reflector (DBR) interference filter (Fig. 1). This architecture ensures a large, constant output angle dependent dispersion (via multilayer periodic layers) that is independent of the input angle (via random nanostructures), allowing it to achieve a huge angular tolerance of 30° with significantly larger optical throughput over 10-fold compared to most compact spectrometers (Table 1). We further engineered the BioDE to disperse light only in the near-infrared (NIR) and transmit visible light without dispersion permitting imaging in the visible (Fig. 1A). These two features, when combined with an imaging lens and a CMOS image sensor, allow the BioDE simultaneously to take a photo in the visible spectrum and perform spectroscopy in the near-infrared (NIR) region in a compact platform including smartphones.

II. Concept and Design of BioDE

The concept of BioDE is illustrated in Fig. 1B. Incident light is first randomly scattered by the 1D scatterers, ensuring the device behaves identically regardless of incident angle of incoming light and thus ensuring angle independent behavior. The angle independent properties of the BioDE is imposed by the complete random distribution of the scatterers. The scattered light is then transmitted through the DBR interference filter. The interference filter consists of two quarter-wavelength stack reflectors of SiO_2 and TiO_2 with an inner SiO_2 cavity layer. To design a NIR spectrometer, the quarter-wavelength layers are engineered to create a stop band through 700 nm to 900 nm wavelength range, with the inner cavity layer acting as a defect

state allowing transmission through the stop band only at a certain resonant wavelength. The transmission wavelength through an interference filter is angle-dependent and is given by:

$$\lambda(\theta) = \lambda_0 \sqrt{1 - \left(\frac{\sin\theta}{n^*}\right)^2} \quad (1)$$

where λ_0 is the transmission at normal incidence, n^* is the effective refractive index, and θ is the output angle. This angle dependent filtering from the interference filter as show in in Eqn. 1 defines the dispersion of BioDE. The magnitude of this dispersion is much larger than what is achievable with a grating, thus permitting the miniaturization of the path length of a BioDE based spectrometer without a significant loss in resolution.

The random density of scatterers (number of nanostructures, distance and distribution) was optimized to maximize the scattering cross-section at 800 nm to a certain angle on the image plane. The resolution and transmission efficiency of a BioDE block were simulated for different numbers of layers in the DBR (Fig. 1C). Increasing the number of layers leads to a higher quality factor (Q) resonance in the filter, thus leading to a higher resolution at the expense of a lower efficiency. For our device, we chose to use 4 layers in the DBR to provide a good balance between the two parameters to achieve 3 nm resolution with 5% efficiency. Different cavity thicknesses leading to different center resonances are used to extend the spectral bandwidth of the chip to 200 nm (Fig. 1D). Since a single BioDE block only scatters at a single angle, multiple BioDE blocks with different cavity thickness are interleaved on a single chip following the long-legged fly eye architecture while scattering at different angles depending on the orientation of the random nanostructures to form a BioDE array (Fig. 1B).

III. Experimental Results

The designed BioDE array was fabricated using standard CMOS-compatible nanofabrication procedures. The final BioDE array, with its 8 individual blocks oriented in different directions for interleaving is presented in Fig. 2A. A zoomed-in image of scanning electron microscopy (SEM) shows the disordered hole pattern that is random in one direction and periodic with subwavelength periodicity in the perpendicular direction. The cross-sectional transmission electron microscopy image shows the DBR stacks below the nanostructures.

The dispersion of the BioDE array was then characterized with a tunable laser setup. To highlight BioDE's ability for high-resolution NIR spectroscopy, the shift in the transmitted intensity with wavelength or wavelength dispersion is shown in Fig 2B. The resolution and average efficiency of the spectrometer are found to be 4.5 nm and 6.6%, respectively.

As mentioned previously, we engineered the BioDE to disperse light only in the NIR and transmit visible light (400nm – 650nm) without dispersion permitting imaging in the visible (Fig. 1). These two features, when combined with an imaging lens and a smartphone camera (CMOS image sensor) (Fig. 3), allow the BioDE simultaneously to capture photo in the visible spectrum and perform spectroscopy in the NIR region. Our imaging target of a Samsung logo shown in Fig. 3B was diffusely illuminated with broadband light, and an image and spectroscopy data was captured via the BioDE array placed in front of a camera. The logo is seen in the center with streaks radially emanating from the center toward the edges, which contain the NIR spectral information. Image processing and spectral reconstruction algorithms are applied to extract the clear image and spectrums computationally. For imaging, we performed a deblurring deconvolution to remove the streaks and make the visible image clear. The spectra was reconstructed using a spectral reconstruction algorithm developed in-house out of the streaks.

To test the spectroscopy ability of the BioDE array, two different filters were added in the light path of the illumination source, and we observed excellent agreement between the BioDE array and the commercial spectrometer as shown in Fig. 3C. We further tested the angle-independent operation of the device to highlight its advantages over commercial spectrometers designed for low acceptance angles (chief ray angles). The spectral intensities measured for an object measured under different incident angles up to 15º with 3º increments are plotted in Fig. 3D. BioDE array has almost constant broadband output across the FOV of 30º (twice the angle of incidence/view) with a variation under 1.7%.

IV. Conclusion

Our work demonstrates a novel bio-inspired dispersion technology (BioDE) that empowers ultracompact spectroscopy in smartphone platform. The combination of large dispersion over 2-fold higher than traditional gratings with the same optics and wide angular tolerance above 30°gives the BioDE based spectrometer the highest signal throughput as well as comparable or better resolution (4.5 nm, up to 0.7 nm possible with this technology) irrespective of the incident light angle and polarization than other miniature spectrometers (Table 1). Spectrometers built with our BioDE platform can collect over 1000 orders of magnitude more light compared to on-chip spectrometers that are based on single/few-mode input waveguides, resulting in much higher sensitivity and performance. Our spectrometer can achieve over 3-fold more signals compared to the current commercial and metasurface based free-space microspectrometers with less thickness.

To our best knowledge, we have shown the first demonstration of high resolution, and wide spectral range spectroscopy in a smartphone with total track length (TTL) ≤ 5 mm. Moreover, the ability to single snapshot capture of 2D visible image and NIR spectra (200 nm, up to 900 nm possible) through high resolution CMOS image sensors allows the direct integration of BioDE onto preexisting optical paths of any camera to turn it into hybrid imager-spectrometer.

This proof-of-concept BioDE technology is envisioned to be integrated into more compact and digital platforms in future, with further improvement in performance through design and algorithm optimization, machine learning and software implementation. We, therefore, envisage a variety of applications enabled by high performance smartphone spectroscopy ranging from face or object detection on mobile platforms, sensing with wearables or implants to general in-situ material characteristics in agricultural, cosmetics and sanitary products by regular consumers.

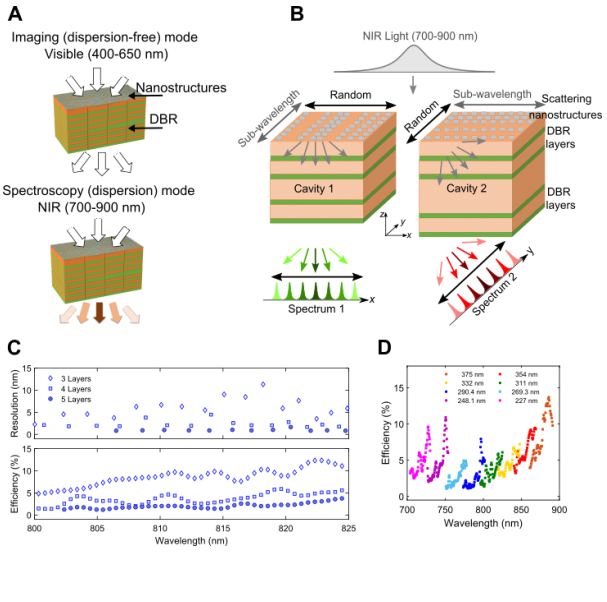

Fig. 1: A) Concept of nanostructured bioinspired dispersion element (BioDE) for single snapshot visible imaging and NIR spectroscopy. B) A schematic of the BioDE design consisting of 2D nanostructures to scatter incident light through a wavelength selective Distributed Bragg reflector (DBR) based interference filter for light dispersion. The scatterers are randomly positioned in one dimension but have subwavelength periodicity in the perpendicular direction to align the light dispersion along a single axis. The orientation of the random nanostructures defines the light dispersion direction. C, D) The interference filter consists of two quarter-wavelength stack reflectors of SiO_2 and TiO_2 with an inner SiO_2 cavity layer. The resolution and efficiency depends on the number of layers in quarter wavelength stack. Depending on the thickness of the cavity layer, the transmission resonance wavelength can be tuned for broadband application.

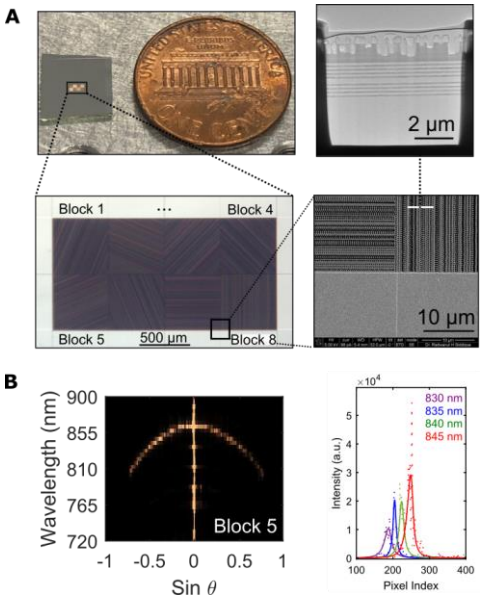

Fig. 2: A) An optical photo of the fabricated BioDE is presented together with a US penny to demonstrate its compact size factor. Scanning electron microscopy (SEM) image shows the intersection of two blocks with orthogonal geometry of controlled disordered nanohole pattern. The cross-sectional transmission electron microscopy (TEM) image confirms the 4 DBR stacks with a cavity inside below the nanostructures. B) The experimental dispersion curve measured from one of the individual blocks of the final BioDE device. One-dimensional intensity profiles shown in the right for several input wavelengths that are 5 nm apart in the bandwidth along the pixels.

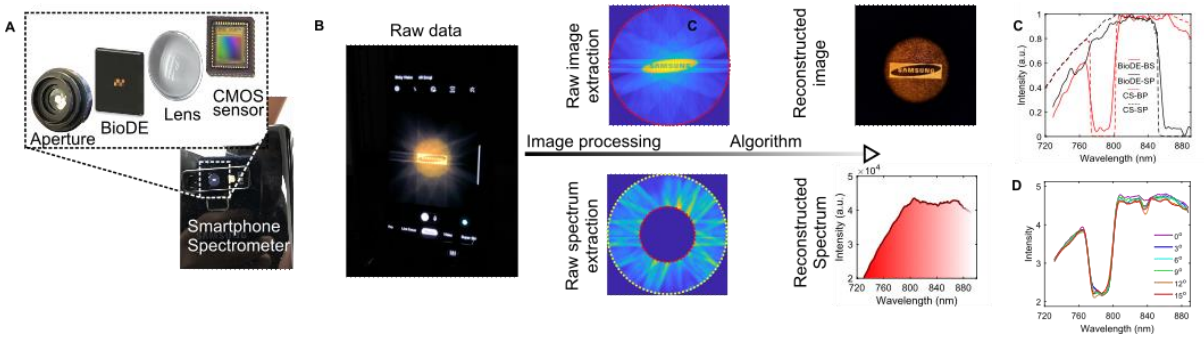

Fig 3. BioDE integration into Smartphone and its imaging and spectroscopy demonstration. A) The schematic of the assembly of the smartphone spectrometer that includes an aperture, BioDE device, an imaging lens and a CMOS image sensor. B) The raw image of a Samsung logo illuminated with a white light source is collected from the smartphone camera. Raw image contains both the image (inner section, field of view (FOV) = 30º) as well as the spectral information (outer section, 30º < FOV < 60º). After series of computational post-processing of the raw image, both the image and the spectrum can be reconstructed. C) Spectrum of a white light source with two different filters, band stop (BS) and short pass (SP) measured by a commercial high resolution spectrometer (CS) and the BioDE empowered spectrometer. D) The spectral intensity is measured under different angles of incidence up to 15º with 3º increments showing negligible variations in the signal under high incident light angles.

Name	Resolution (nm)	Efficiency (%)	Range/Bandwidth (nm)	Field-of-view (°)	Input Aperture (Scalability)	Optical Entendue (Area * 4*pi*Sin(theta/2)^2 (Srum^2)	Maximum Achievable Signal (Entendue * Efficiency) (Srum^2)	Simultaneous Imaging	Total track length/ system thickness (mm)
This work	**4.5/0.7(max)**	**6.6/18(max)**	**200/ 900 (max)**	**30x30**	**2mmx1mm (Yes)**	**4.30E+05**	**3500**	**Yes**	**≤ 5**
Micro-optical spectrometer (*3*)	12	37.5	410	25x25	50umx500um (No)	3.7E+03	1400	No	20
Single-nanowire spectrometer (*14*)	7	NA	130	NA	NA	NA	NA	No	>10
A colloidal quantum dot spectrometer (*13*)	3.2	NA	300	NA	NA	NA	NA	No	NA
Metasurface Spectrometer (*5*)	1.1	25	100	2x0.3	Diameter of 790 um (No)	90	22.5	No	7
On-chip photonic crystal slabs spectrometer (*12*)	1.5	NA	200	1x1	210um x 210um (Yes)	609	NA	No	>35
Disordered nanophotonic on-chip spectrometer (*7*)	0.75	NA	25	NA	NA	<0.5	<0.5	No	NA
Arrayed waveguide grating spectrometers (*11*)	1	23	10	NA	NA	0.8	0.2	No	16
Reconfigurable metasurface slab spectrometer (*16*)	0.8	NA	300	NA	NA	NA	NA	Yes	>10

Table 1. Comparison of this work with a range of demonstrated microspectrometer technologies from the literatures as well as one that is commercially available. We have highlighted the best numbers in green.

References

[1] Savage, N.. *Nat. Photonics* **3**, 601 (2009)
[2] McGonigle, A. J. S. et al. *Sensors* **18**, 223 (2018)
[3] Hamamatsu mini-spectrometer micro series C12666MA (2015)
[4] Shibayama, K., Suzuki, T. & Ito, M. Spectroscope. (2013)
[5] Faraji-Dana, M. et al. *Nat. Communications*. **9**, 4196 (2018)
[6] Momeni, B., Hosseini, E. S., Askari, M., Soltani, M. & Adibi, A. *Opt. Commun.* **282**, 3168–3171 (2009)
[7] Redding, B., Liew, S. F., Sarma, R. & Cao, H. *Nat. Photonics* **7**, 746 (2013)
[8] Xia, Z. et al. *Opt. Express* **19**, 12356–12364 (2011)
[9] Velasco, A. V et al. *Opt. Lett.* **38**, 706–708 (2013).
[10] Wang, S.-W. et al. *Opt. Lett.* **32**, 632–634 (2007).
[11] Horie, Y., Arbabi, A., Arbabi, E., Kamali, S. M. & Faraon, A. *Opt. Express* **24**, 11677–11682 (2016).
[12] Wang, Z. et al. *Nat. Commun.* **10**, 1020 (2019).
[13] Bao, J. & Bawendi, M. G. *Nature* **523**, 67 (2015).
[14] Yang, Z. et al. *Science* **365**, 1017 LP – 1020 (2019).
[15] Stavenga, D. G. et al. *J. Comp. Physiol. A* **203**, 23–33 (2017)
[16] J. Xiong, et arXiv preprint arXiv:2005.02689 (2020).